Full Title: Monitoring and responding to emerging infectious diseases in a university setting: A case study using COVID-19

Short title: Monitoring and responding to emerging infectious diseases in universities

K. James Soda[1*], Xi Chen[2], Richard Feinn[3], David R. Hill[3]

[1]Department of Mathematics and Statistics, Quinnipiac University, Hamden, Connecticut, USA

[2]Department of Sociology and Anthropology, Quinnipiac University, Hamden, Connecticut, USA

[3]Department of Medical Sciences, Frank H. Netter MD School of Medicine, Quinnipiac University, Hamden, Connecticut, USA

* Corresponding author

E-mail: Kenneth.Soda@quinnipiac.edu

Abstract

Emerging infection diseases (EIDs) are an increasing threat to global public health, especially when the disease is newly emerging. Institutions of higher education (IHEs) are particularly vulnerable to EIDs because student populations frequently share high-density residences and strongly mix with local and distant populations. In fall 2020, IHEs responded to a novel EID, COVID-19. Here, we describe Quinnipiac University's response to SARS-CoV-2 and evaluate its effectiveness through empirical data and model results. Using an agent-based model to approximate disease dynamics in the student body, the University established a policy of dedensification, universal masking, surveillance testing via a targeted sampling design, and app-based symptom monitoring. After an extended period of low incidence, the

infection rate grew through October, likely due to growing incidence rates in the surrounding community. A super-spreader event at the end of October caused a spike in cases in November. Student violations of the University's policies contributed to this event, but lax adherence to state health laws in the community may have also contributed. The model results further suggest that the infection rate was sensitive to the rate of imported infections and was disproportionately impacted by non-residential students, a result supported by the observed data. Collectively, this suggests that campus-community interactions play a major role in campus disease dynamics. Further model results suggest that app-based symptom monitoring may have been an important regulator of the University's incidence, likely because it quarantined infectious students without necessitating test results. Targeted sampling had no substantial advantages over simple random sampling when the model incorporated contact tracing and app-based symptom monitoring but reduced the upper boundary on 90% prediction intervals for cumulative infections when either was removed. Thus, targeted sampling designs for surveillance testing may mitigate worst-case outcomes when other interventions are less effective. The results' implications for future EIDs are discussed.

Introduction

Emerging infectious diseases (EIDs) increasingly pose a threat to global public health. An EID is any pathogenic disease that has been newly introduced to an area or whose incidence has rapidly increased (1,2). Even after correcting for differences in sampling effort, EIDs have originated at an increasing rate since 1940 (3). Modern trends in global connectivity, population growth, and interactions at the human-environment interface are all theorized to contribute to the growth of EIDs by accelerating the rate at which local outbreaks can propagate globally (4,5). Novel diseases are an especially problematic subcategory of EIDs because there is no existing literature for these diseases on which public health officials can inform their responses. To reflect the threat of novel pathogens, the World Health Organization has placed Disease X on its list of priority diseases for research and public health planning

since 2015 (6). The Disease X designation is a placeholder for a yet unknown pathogen with the capacity to cause a global pandemic, and is intended to encourage the scientific and public health communities to develop response plans that can apply to non-specific pathogens (7). The Disease X concept became a reality in 2020 as the novel SARS-CoV-2 virus led to the ongoing COVID-19 pandemic. In light of concerns that new strains of coronaviruses or similar respiratory infections (*e.g.*, influenza) could cause the next global pandemic (5,8), it is critical that the public health community take stock of what measures were most effective in early COVID-19 responses in order to prepare for the next EID or Disease X.

Institutions of higher education (IHEs) pose unique public health challenges in the face of EIDs with droplet and airborne transmission, in part due to how most university-owned properties are structured. Most university-owned residences feature high densities of students living in individual rooms with high densities of rooms on each floor, which can accelerate disease transmission (9,10). Further, lavatory facilities in many university residences are shared between several rooms. This poses an additional challenge because basic hygiene practices, such as bathing and dental care, preclude masking, and surfaces such as faucets and door handles facilitate fomite transmission when applicable. Finally, transmission is likely to jump between university residences as their occupants intermingle at shared facilities (e.g., food services, athletic facilities, libraries) and in the classroom.

Further, university-owned residences are differentiated from other residential facilities (*e.g.*, hospitals, long-term care facilities, prisons) through the multiscale population mixing that is inherent to campus communities. On a local level, university students regularly mix with surrounding communities through student employment, peers in off-campus housing, interactions with friends and family outside of the university, and participation in community events. Additionally, most IHEs include students originally from populations beyond those surrounding the campus. This means that student populations can be expected to mix at intra- and international scales, especially at the beginning and end of semesters and following major holidays. This increased mixing can pose a double threat to infection containment. On the one hand, mixing could cause infections to spill over from IHEs into connected populations. On the

other hand, mixing can introduce infections into an IHE's population, where the previously discussed factors can amplify disease transmission.

Quinnipiac University is a suburban university located in New Haven County, Connecticut, USA. In the fall 2020, the University had 6,841 undergraduate students and 2,903 graduate students (11). The University allowed students to attend classes via an online-only or hybrid (*i.e.*, partially in-person and partially online) modality. Approximately 7,100 students selected the hybrid modality. Roughly 55% of undergraduates lived on campus (11). University-owned residences included 15 dormitories, 10 townhouses, and 53 free-standing houses that ranged in size from two to four bedrooms.

In preparation for the 2020/2021 academic year, the University established a COVID-19 task force charged with developing a plan to allow in-person and remote instruction while minimizing the risk of COVID-19 transmission. Like other institutions (*e.g.*, (12–15)), Quinnipiac de-densified classrooms to allow physical distancing and required facemask usage in most public spaces. The maximum capacity in university residences was reduced to no more than two students per room. To facilitate remote learning, classrooms were equipped with specialized audio-visual equipment, and professors at high risk for severe illness were allowed to teach online. The task force's plan also emphasized student testing protocols to detect COVID-19 cases, and instituted isolation, quarantine, and contact tracing protocols upon case identification. The testing protocols used both random surveillance testing and symptom-based monitoring. To assist symptom-based monitoring, the University distributed a smart-phone application that logged the user's COVID-related symptoms each day and instructed the user to seek testing when their symptoms suggested COVID-19 infection. The COVID-19 protocols required additional, fine-grained decisions, such as the number of rooms needed for isolation and quarantine, the number of contact tracers required to follow transmission chains, and the optimal strategy for sampling students for surveillance testing. Because SARS-CoV-2 was a Disease X scenario, there was little data to inform these decisions. To address this knowledge gap, the task force formed a subcommittee to develop a model of how COVID-19 could spread through the student body during the fall semester based on available

knowledge about SARS-CoV-2 transmission, contact patterns in college-aged individuals, and the spatial structure of university-owned residences. The modeling team worked on the premise that not all students needed to be tested to reliably identify COVID-19 circulation amongst the student body.

The modeling subcommittee used an open-source agent-based model for community COVID-19 dynamics, Covasim, as a basis for their model, but modified Covasim to better reflect the nested housing structure found in university-owned residences (16). An agent-based model simulates a system using computational units, called agents, that interact with each other based on well-defined rules and seeks to explore what patterns arise in the simulation that are not immediately predictable based on the agents' individual actions (17). Agent-based models are well-suited to inform policy decisions because they provide a granular depiction of their populations and explicitly simulate the behavior of individuals. As a result, individual-based interventions, such as contact tracing, and traits, such as contact networks, are more easily translated into the model. Covasim has been used to guide primary and secondary school reopening strategies in the United States and the United Kingdom (18–21) and was similarly adapted to guide public health policy at Boston University (22). However, this was the first use of the adapted form developed at Quinnipiac.

In this paper, we detail what modifications we made to Covasim to better simulate a university's student body in general and Quinnipiac University in particular. We also describe Quinnipiac's COVID-19 testing protocol, particularly the survey methodology design used to sample students for surveillance testing. Finally, we compare the performance of the model against the actual case numbers during the fall semester of 2020, evaluate the effectiveness of the University's protocols, and discuss its implications for university responses to future Disease X scenarios.

Materials and methods

Covasim model

Our model extended the Institute for Disease Modeling's Covasim model (16). Covasim is a stochastic, agent-based model of COVID-19 dynamics that assigns one agent to each individual or set of identical individuals. In our implementation, each agent represented one student. The model builds on a discrete-time susceptible-exposed-infectious-recovered model, but its agent-based structure allows it to explicitly incorporate relevant interhost properties, such as viral loads, age-dependent susceptibility and transmissibility, and heterogeneity in susceptibility, transmissibility, and recovery times. The model also organizes agents into sets of pools, each representing a different social context (*e.g.*, home, work, and school). On each day, every individual forms a new contact network by sampling a Poisson-distributed number of agents from its pools, thus allowing the model to simulate heterogeneous population mixing through pool membership. Disease transmission randomly occurs when an infectious individual contacts a susceptible individual. The probability of transmission depends on the pool associated with the contact and on the current properties of each agent (*e.g.*, infectious host's viral load). Covasim assigns an outcome to each infection, such as whether symptoms develop, and every infection may be diagnosed through testing. The version of the Covasim model that we used, including the added features discussed here, are available through GitHub (https://github.com/kjamessoda/covasim.git) and within the F20ModelAndTesting branch.

Contact network structure

We modified Covasim's contact pools so that the pools better emulated the structure of university-owned residences. Contact pools focused on housing structure rather than classroom structure because we assumed that the University's physical distancing and masking policies would lower transmission rates within the classroom to a negligible level. This assumption was later confirmed through contact tracing data, and has been borne out in other university settings (23). Contact pools fell into four categories: community, floor, bathroom, and room. Every agent belonged to a single community pool. Then, subsets of the community pool formed floor pools, each representing students living on the

same floor of a dormitory or in a comparable unit of a university-owned residence. In turn, subsets within each floor pool formed bathroom pools, each representing students who shared the same bathroom, and subsets within the bathroom pools formed room pools, each representing a single set of roommates. A single room pool represented students living in free-standing houses. The mean number of contacts drawn from each pool to create a contact network could differ between pools (see Simulation Setup). Room pools were the exception to this rule; each agent's contact network contained their roommates every day, an assumption that both the University's contact tracing data and reports from other universities subsequently validated (9).

To account for students living outside of university-owned housing, agents were divided into residential students and non-residential students. Non-residential students at Quinnipiac lived in diverse housing arrangements (*e.g.*, cohabitating with other students, living with family members), so we did not represent their contact networks using floor, bathroom, and room pools. The community pool, however, functioned in the same manner for both student types.

Imported infections

To represent disease transmission from non-students to students, the model randomly selected agents to potentially transition to the exposed compartment without contacting an infectious student (*i.e.*, an imported infection). Although exposed, infected, and recovered agents were eligible for selection, only susceptible agents transitioned. Residential and non-residential students were sampled separately each day, and the number of agents sampled was a Poisson random variable whose mean was proportional to the size of the agent group, the expected number of non-student contacts per student, and the estimated prevalence of COVID in Connecticut (see Simulation Setup; S1 Appendix).

Conversion from R_0 to probability of transmission

Covasim does not explicitly use the basic reproductive number (R_0) as a model parameter. The closest analog is the base probability of transmission (β). Nonetheless, it is possible to extend Covasim's assumptions to relate an *a priori* value for R_0 to β (S1 Appendix). R_0 is defined as the expected number of new infections in a fully susceptible, well-mixed population after a single infectious individual is introduced. If the age structure of the population emulates that of the United States (24) (though see Table A in S1 Appendix for a minor deviation), then Covasim's models of viral load dynamics and disease transmission imply:

$$\beta \approx \frac{R_0}{8.093758 n_c}$$

where n_c is the expected number of contacts one individual has in one day.

Interventions

Covasim provides testing-based public health interventions and contact tracing interventions (16). Testing-based interventions receive a set of agents and change infected agents to the diagnosed state based on a provided test sensitivity. We set the sensitivity to 0.95 to emulate nasal swab PCR tests for SARS-CoV-2 virus (25). The model had a one-day delay between testing and diagnosis. Upon diagnosis, individuals were transferred to isolated populations and made no further contacts until entering the recovered compartment. Each diagnosis also led to a reported case in the model's output. Testing-based interventions differed in how the sets of individuals to test were generated.

We implemented three testing-based interventions in our simulations, each corresponding to one of the University's public health interventions. In fall 2020, every member of Quinnipiac University, including students, was asked to complete a daily public health application that screened for COVID-19 symptoms (MyOwnMed COVID-19 symptom application; MyOwnMed, Inc. Bethesda, Maryland 20817). Students with symptoms were asked to contact Student Health Services, be evaluated, receive a COVID-19 test, and isolate until the results returned. Student Health Services also monitored the

symptom application dashboard and contacted students who reported COVID-19-like symptoms for further evaluation. To simulate the application's impact, each day a symptom-monitoring intervention identified symptomatic agents in the simulation who had not been tested for COVID-19. The intervention transferred these students to the isolated population and tested them using the procedures above. If the student tested negative for SARS-CoV-2, they returned to the general population after the one-day delay. To account for imperfect app usage, we set the daily probability of detection to 0.5, corresponding to an expected one-day delay between symptom onset and detection. In addition to symptom-monitoring, the University randomly tested residential students based on a targeted sampling design and non-residential students using a simple random sample (SRS) (see Sampling Strategy). Since the model integrated the structure of university residences into its contact networks and differentiated students by housing status, we designed a second testing-based intervention to replicate the targeted design for residential students and a third to replicate the SRS for non-residential students.

Contact tracing interventions were carried out by university contact tracers. To reflect this, after a testing-based intervention moved an infectious agent into isolation, a contact-tracing intervention retrieved the infectious individual's contact network and quarantined its contacts to the isolated population. In our implementation, contact tracing always successfully identified roommate contacts, but all remaining contacts had a 0.75 probability of identification. To be cautious, there was a two-day delay within the simulation between when contact tracing started and when identified contacts moved to isolation; however, real tracing usually required less time. Quarantined individuals reentered the general population after 14 days if they tested negative for SARS-CoV-2 virus and after entering the recovered compartment if they tested positive.

Simulation setup

We simulated COVID-19 dynamics in the University's student body between Aug. 31 and Nov. 24, 2020, the period between the beginning of classes and the Thanksgiving holiday; nearly all university

students remained at home following Thanksgiving. Every simulation contained 3,636 residential students, each associated with a university property through their contact network structure (see Contact Network Structure), and 3,789 non-residential students, leading to a total population of 7,425 students. These population sizes slightly differ from the actual population sizes in fall 2020, which were unavailable during the summer. Every agent was randomly assigned an age between 18 and 22. Each simulation implemented the four interventions above (*i.e.*, app-based symptom monitoring, targeted surveillance testing of residential students, simple random surveillance testing of non-residential students, and contact tracing). In accordance with the University's testing schedule, the surveillance testing interventions ran on every simulated Tuesday and Wednesday. The symptom monitoring and contact tracing interventions ran daily. We estimated Connecticut's COVID-19 prevalence to be roughly 2.8 infectious individuals per 1,000 residents based on the statewide case incidence between Aug. 30 and Sept. 2, 2020 (S1 Appendix). This estimate informed the rate of imported infections in the simulations.

We simulated four main scenarios, each pairing one of two R_0 values (see Conversion from R_0 to Probability of Transmission), 1.5 or 2.5, and one of two average contact rates, 8 contacts/day or 10 contacts/day. Bharti *et al.* (26) informed the contact rates. Table 1 lists how the contacts were allocated across pools. Since non-residential students only belonged to the community pool, we allocated their remaining contacts to non-students under the assumption that non-residential students would mix more with the surrounding community. The rate of imported infections under each scenario was established based on the scenario's probability of transmission and average contact rate (Table 2; S1 Appendix). Every scenario was run 1,000 times to generate a distribution of possible outcomes. The median outcome on each day was used as a prediction, and the 5^{th} and 95^{th} percentiles provided a 90% prediction interval.

Table 1. Average number of contacts per day from each pool under two total contact rates.

	8 contacts/day		10 contacts/day	
Pool	**Residential**	**Non-Residential**	**Residential**	**Non-Residential**
Community	2.5	2.5	4	4
Floor	2	-	2	-

Bathroom	3	-	3	-
Room	Full Pool	-	Full Pool	-
Non-Student	0.5	5.5	1	6

Table 2. The rate of imported infections (in infections/week) under four scenarios with different basic reproductive numbers (R_0) and average contact rates.

			Average Contact Rate (contacts/week)	
			8	*10*
Residential	**R_0**	*1.5*	0.8279664	1.324746
		2.5	1.379944	2.207910
Non-Residential	**R_0**	*1.5*	9.490872	8.282943
		2.5	15.81812	13.80490

Although it did not inform policy, we also assessed model sensitivity to the rate of imported infections by rerunning each main scenario with half and twice the rates provided in Table 2. Since there were initially no infected individuals in the simulations, every transmission chain must begin with an imported infection. Assuming that the expected number of infections in every transmission chain is constant given residential versus non-residential designation and that the susceptible pool does not become significantly depleted, the expected number of infections at the end of a simulation should be proportional to the rate of imported infections. We therefore measured the model's sensitivity to the rate of imported infections as the scaling constant on this relationship as estimated using a least-squares line through the median predictions that is constrained to pass through the origin. Least-squares lines were fit

using routines in the SciPy Python library (27,28). Python code to implement each scenario is available in S2 Additional Material.

Sampling strategy for surveillance testing

To minimize the risk of initial spread, every student completed a PCR test for SARS-CoV-2 prior to coming to campus in August 2020 and again within two weeks of campus arrival. Subsequently, students were randomly sampled for testing. The student body was divided into four categories: residential students, non-residential undergraduates, non-residential graduate students, and student athletes (S1 Appendix).

Most Quinnipiac students were residential students. For these students, we applied a targeted sampling design that combined strict stratified and cluster sampling methods. We defined building floors and off-campus houses as strata and determined the number of students to select from each stratum. Guided by model results, the sampling rate for each stratum was initially 15%. The choice of 15% gave the university the highest likelihood of detecting an outbreak, without having to test all students. Although a stratified sampling strategy would reduce the standard error on any resulting incidence estimate, our goal was to increase the likelihood of detecting an outbreak through even sampling coverage across floors, suites, and houses, rather than estimating epidemiological parameters. After establishing the sample size for each stratum, we used a cluster sampling method to randomly select students to test. Each cluster was a dorm room or suite. First, SRS selected the appropriate number of dorm rooms or suites for each stratum; then one student was sampled from each selected dorm room and suite through SRS. Such an approach maximized the number of dorm rooms and suites being selected.

We used more traditional sampling designs for the remaining three student sub-populations. The sampling rate for student athletes was initially 80% and was stratified by team (*e.g.*, men's hockey, woman hockey, *etc*.). Non-residential undergraduate and graduate students were generally selected via SRS and initially at 25% and 15%, respectively, although each week's sample had to contain at least one

student from every address that housed three or more students. As the semester progressed, we adapted each subpopulation's sampling rate in response to trends in the observed case incidences (Table B in S1 Appendix).

Comparison of sampling strategies

To assess the efficacy of our targeted sampling design for surveillance testing, we compared our model's predicted infection trajectory under the targeted design to an SRS design and to complete sampling. To make the SRS design more comparable to the targeted design, the SRS scenarios randomly sampled 355 students on Tuesdays and 225 students on Wednesdays. Due to rounding error at each stratum and the desire to split surveillance testing across two days, the targeted design used these same sample sizes before accounting for individuals in quarantine or isolation. The complete sampling scenarios evenly split surveillance tests between Tuesdays and Wednesdays. We compared these three strategies under the four main scenarios described in Simulation Setup.

To further explore the relationship between sampling designs for surveillance testing and other public health interventions, we also ran holdout scenarios where contact tracing or app-based symptom monitoring were withheld. Since targeted sampling was only used on residential students, each holdout scenario solely simulated residential students. We also ran a baseline all-interventions scenario where all interventions were used to assess the impact of removing non-residential students from the simulation. There were two holdout scenarios for app-based symptom monitoring. In the app-based symptom monitoring intervention, the expected waiting time between when an individual developed symptoms and when the individual sought testing was one day to reflect the application's impact. To assess how each sampling design might have performed in the absence of app-based monitoring, we changed the expected waiting time to 4.82 days, the estimated mean waiting time between symptom onset and first clinical visit in Khalili *et al.* (29). We called this the delayed-symptom-testing scenario. As an upper extreme, we also ran a scenario with no symptom-based monitoring (*i.e.*, all testing was surveillance testing). In all holdout

298 scenarios, R_0 was 2.5, and the average contact rate was 10 contacts/day. These holdout scenarios also
299 provided guidance on the impact of individual interventions and the role of non-residential students in
300 disease transmission.

301 As with the main scenarios, 1,000 simulations comprised each holdout scenario. We assessed the
302 differences between holdout scenarios based on their median cumulative infections across simulations and
303 on their 90% prediction intervals (*i.e.*, 5^{th} and 95^{th} percentiles). Python code to implement each sampling-
304 strategy and holdout scenario is available in S2 Additional Material.

305 Ethics Statement

306 Quinnipiac University's Institutional Review Board determined that the surveillance sampling
307 design detailed here fell under the category of public health surveillance and not research, and thus, the
308 design did not require further board consideration. All case incidence data reported here was used
309 retrospectively and was fully anonymized before the researchers accessed it. Therefore, this data does not
310 fulfill the US Office for Human Research's definition of human subject data.

311 Results

312 Adjustments to sampling strategy

313 Throughout the fall semester, we adjusted the proportion of students sampled in each category
314 (*i.e.*, residential undergraduates, non-residential undergraduates, non-residential graduate students, and
315 student athletes) based on their observed case incidences. The testing proportions were determined by the
316 modeling subgroup and the university COVID-19 taskforce.

317 Following universal testing of students prior to and within two weeks of arrival, we implemented
318 surveillance testing based on model results. Beginning on the third week, 25% of non-residential

undergraduates, 15% of graduate students and residential undergraduates, and 80% of student athletes were selected for testing. If a student tested positive, they were removed from the sampling frame for 90 days under the assumption that they had acquired natural immunity and based in Centers for Disease Control and Prevention guidance that did not recommend PCR testing within 90 days of confirmed infection (30). In response to an increase in cases beginning in October, the sampling rate for non-residential students was adjusted to 35%. Following a super-spreader event in late October that caused a marked increase in cases during the first week of November, the University increased the proportion of students tested and implemented new mitigation policies, including switching to online course instruction and restricting all students to their dormitories for 14 days. In the second week of November, every student was tested. A limited number of in-person classes resumed the week before Thanksgiving. In line with most other IHEs, students remained home after the Thanksgiving Break and classes continued remotely.

Observed incidence rate and main-scenarios comparison

There was a total of 613 reported COVID-19 cases at Quinnipiac University between September 16, 2020, and Nov. 24, 2020 (Fig 1). Cases were not evenly distributed across this period. Before October 11, there were only six reported cases. The infection rate gradually increased through October before an off-campus super-spreader event at the end of the month led to 495 cases between Nov. 1 and Nov. 6.

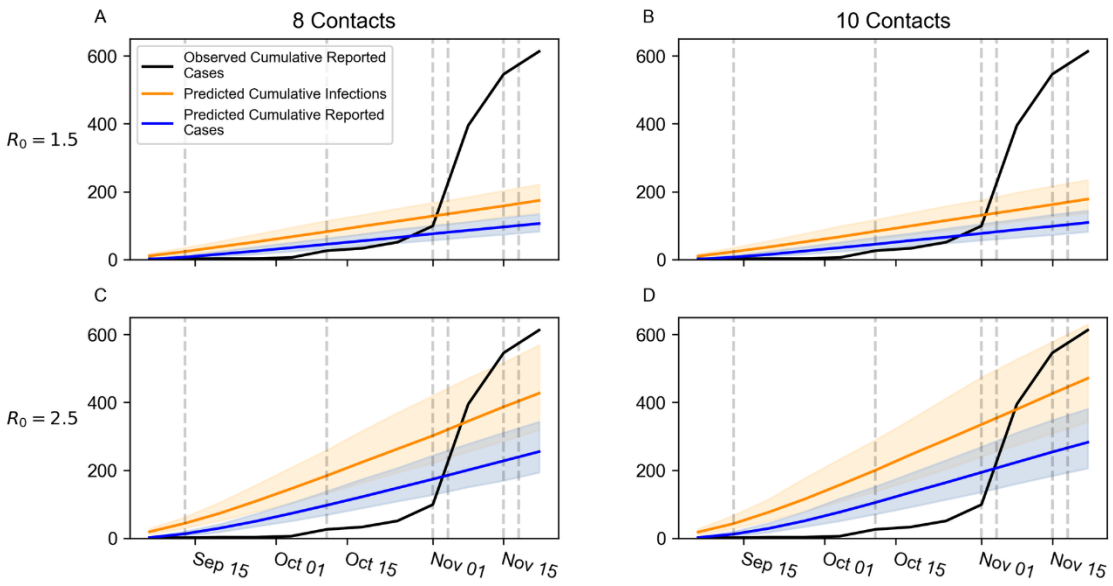

Fig 1. Predicted cumulative infections and reported cases under four scenarios compared to the observed cumulative cases. Solid, colored lines represent the median prediction across 1,000 replicate simulations. Shaded regions represent 90% prediction intervals spanning the 5th and 95th percentiles. Predicted cumulative infections are depicted in orange. Predicted cumulative reported cases are depicted in blue. Solid black lines depict observed cumulative reported cases. Vertical dashed lines indicate dates where the sampling scheme was adjusted. A) $R_0 = 1.5$, 8 contacts/day, B) $R_0 = 1.5$, 10 contacts/day, C) $R_0 = 2.5$, 8 contacts/day, D) $R_0 = 2.5$, 10 contacts/day.

The fit between the observed case incidence and those predicted by the model also changed through time. Until Nov. 8, the $R_0 = 1.5$ scenarios fit the observed cumulative cases relatively well, with the 10 contacts/day scenario performing slightly better than the 8 contacts/day scenario (Fig 1). The observed cases fell within the $R_0 = 1.5$, 10 contacts/day scenario's prediction intervals on Sept. 6 and between October 25 and November 1. Although the observed cumulative cases between September 13 and October 18 were below this scenario's prediction intervals, the difference between the observed cases and the interval's lower boundary was no more than six cases between September 13 and September 20

and between October 11 and October 18. After Nov. 1, no scenario's prediction interval for diagnosed cases contained the observed cumulative cases. However, the observed cumulative cases fell within the R_0 = 2.5, 10 contacts/day scenario's prediction interval for total infections throughout this period.

Qualitatively, the model predicted steady increases in the case incidence under all four scenarios. The epidemiological trajectory in the R_0 = 1.5 scenarios were similar, regardless of the contact rate, whereas the contact rate differentiated the R_0 = 2.5 scenarios to a more noticeable degree. This same pattern occurred in each scenario's final median cumulative infections (R_0 = 1.5, 8 contacts/day: 178 infections, R_0 = 1.5, 10 contacts/day: 182 infections, R_0 = 2.5, 8 contacts/day: 438 infections, R_0 = 2.5, 10 contacts/day: 484 infections). In contrast, the observed cumulative cases increased at a heterogenous rate. Early in the semester, there were few observed cases. Beginning in October, the cumulative incidence began to rise at a greater, though still largely steady, rate. After the super-spreader event, the cumulative incidence sharply increased and grew nonlinearly.

Sensitivity analysis for the rate of imported infections

To assess how the rate of imported infections impacts the model's epidemiological trajectory, we repeated all four scenarios but scaled the rate of imported infections by one half and two relative to the values in Table 2. As expected, the median total infections in each scenario was roughly proportional to the rate of imported infections (Fig 2). The proportional relationship is stronger when R_0=1.5 than when R_0=2.5. The estimated scaling constant for this relationship was similar between the R_0=1.5 scenarios (R_0=1.5, 8 contacts/day: 17.10; R_0=1.5, 10 contacts/day: 18.67). The estimated scaling constants for the R_0=2.5 scenarios were greater in magnitude than in the R_0=1.5 scenarios and were better differentiated between contact rates (R_0=2.5, 8 contacts/day: 24.12; R_0=2.5, 10 contacts/day: 27.63).

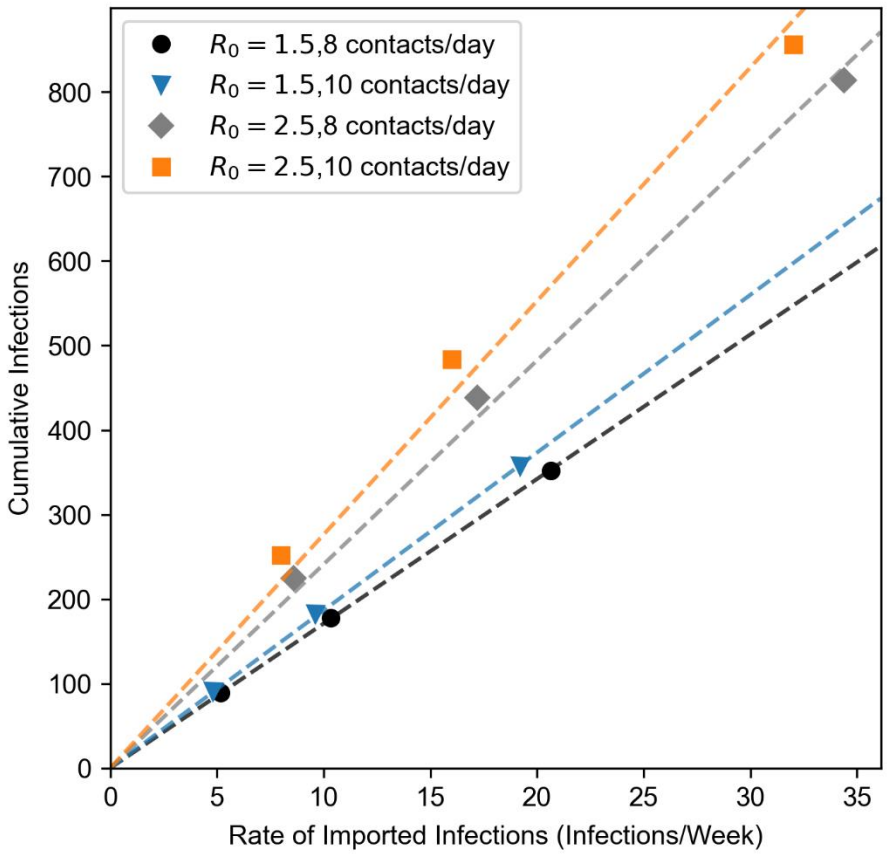

374

375 **Fig 2. Median cumulative infections against rate of imported infections under four epidemiological**
376 **scenarios.** Dashed lines represent the least-squares line for its corresponding scenario, constrained to pass
377 through the origin. Black circles: R_0=1.5, 8 contacts/day, blue triangles: R_0=1.5, 10 contacts/day, grey
378 diamonds: R_0=2.5, 8 contacts/day, orange squares: R_0=2.5, 10 contacts/day

379

380 Comparison of sampling strategies

381 Predictions for final cumulative infections differed minorly to moderately across targeted testing,
382 SRS, and complete sampling when R_0 =1.5 (Fig 3 A, B). The median predictions for targeted testing and

383 SRS differed by no more than three infections, whereas the difference between complete sampling and
384 targeted sampling was 19 infections under 8 contacts/day and 24 infections under 10 contacts/day. The
385 lower boundaries on the 90% prediction intervals (*i.e.*, 5th quantile) differed less. No more than 16
386 infections separated the lower boundary of any design under either scenario. The differences between
387 complete sampling and the random sampling strategies were more pronounced in the 90% predictions
388 intervals' upper boundaries (*i.e.*, 95th quantile). Relative to targeted sampling, complete sampling had
389 32.05 fewer infections at the under boundary under 8 contacts/day and 44 fewer infections under 10
390 contacts/day. In contrast, targeted sampling and SRS had very similar upper boundaries that differed by
391 no more than three infections.

392

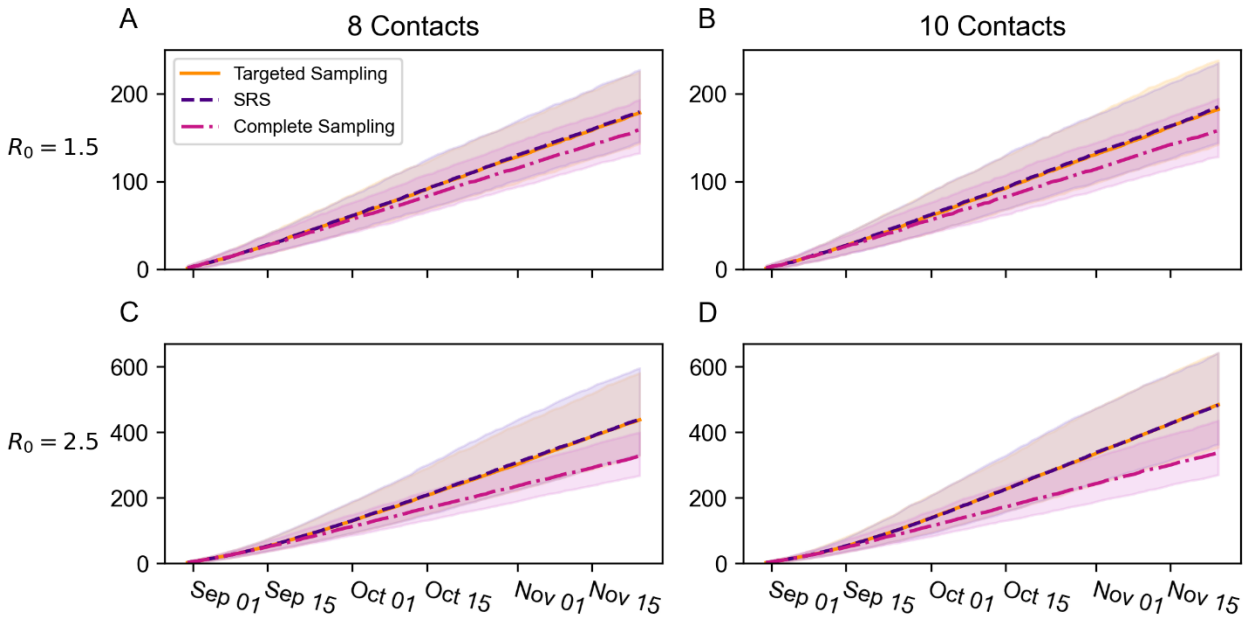

393

394 **Fig 3. Comparison of three sampling designs for surveillance testing under four epidemiological**
395 **scenarios.** Solid and dashed lines represent the median cumulative infections across 1,000 replicate
396 simulations. Shaded regions represent 90% prediction intervals spanning the 5th and 95th percentiles.
397 Targeted sampling is depicted in orange. Simple random sampling (SRS) is depicted in purple. Complete

398 sampling is depicted in magenta. A) $R_0 = 1.5$, 8 contacts/day, B) $R_0 = 1.5$, 10 contacts/day, C) $R_0 = 2.5$, 8
399 contacts/day, D) $R_0 = 2.5$, 10 contacts/day

400

401 When $R_0 = 2.5$, complete sampling led to many fewer infections relative to the random sampling
402 strategies (Fig 3 C, D). In the $R_0 = 2.5$, 8 contacts/day scenario, the median cumulative infections was 110
403 infections lower under complete sampling relative to targeted sampling and was 146 infections lower in
404 the $R_0 = 2.5$, 10 contacts/day scenario. Once again, the upper boundaries on the 90% confidence intervals
405 showed even more pronounced differences between complete sampling and targeted sampling (8
406 contacts/day: 182 infections, 10 contacts/day: 206.85 infections). The differences between targeted
407 sampling and SRS, however, were comparably minor. The median predictions differed by no more than
408 two infections and the lower boundaries on the prediction intervals differed by no more than 9.05
409 infections. The greatest difference between these two scenarios occurred in the upper boundary under 8
410 contacts/day (15 fewer infections under targeted testing). The difference was minute, however, when
411 there were 10 contacts/day (one fewer infection under targeted testing).

412 Under most holdout scenarios, the median cumulative infections and lower boundaries on the
413 90% prediction intervals differed very little between targeted sampling and SRS (Fig 4). On the last day
414 of the simulation, the medians and the lower boundaries for targeted sampling and SRS were all within
415 three cases of each other under the all-interventions, no-contact-tracing, and delayed-symptomatic-testing
416 scenarios. The no-symptomatic-testing scenario was the exception. In this case, the median prediction for
417 SRS was 19 infections greater than that for targeted sampling, and the lower boundary on SRS's
418 prediction interval was 83.3 infections greater than that of targeted sampling. In contrast, targeted
419 sampling had 90% confidence intervals with noticeably lower upper boundaries than SRS under every
420 holdout scenario (all-interventions: 14.0 infections, no-contact-tracing: 19.2 infections, delayed-
421 symptomatic-testing: 18.0 infections, no-symptom-monitoring: 38.8 infections). The difference between

the two strategies' upper boundaries displayed an upward global trend through time. This may indicate that the difference between the two strategies would have become even more pronounced if the simulations were allowed to continue, although each scenario had a declining local trend on the simulation's last day. It is also worth noting that there was substantial variation in how many infections were predicted in each scenario. Under targeted sampling, the all-intervention scenario had 139 infections, the no-contact-tracing scenario had 212.5 infections, the delayed-symptomatic-testing scenario had 318.5 infections, and the no-symptomatic testing scenario had 1,458 infections.

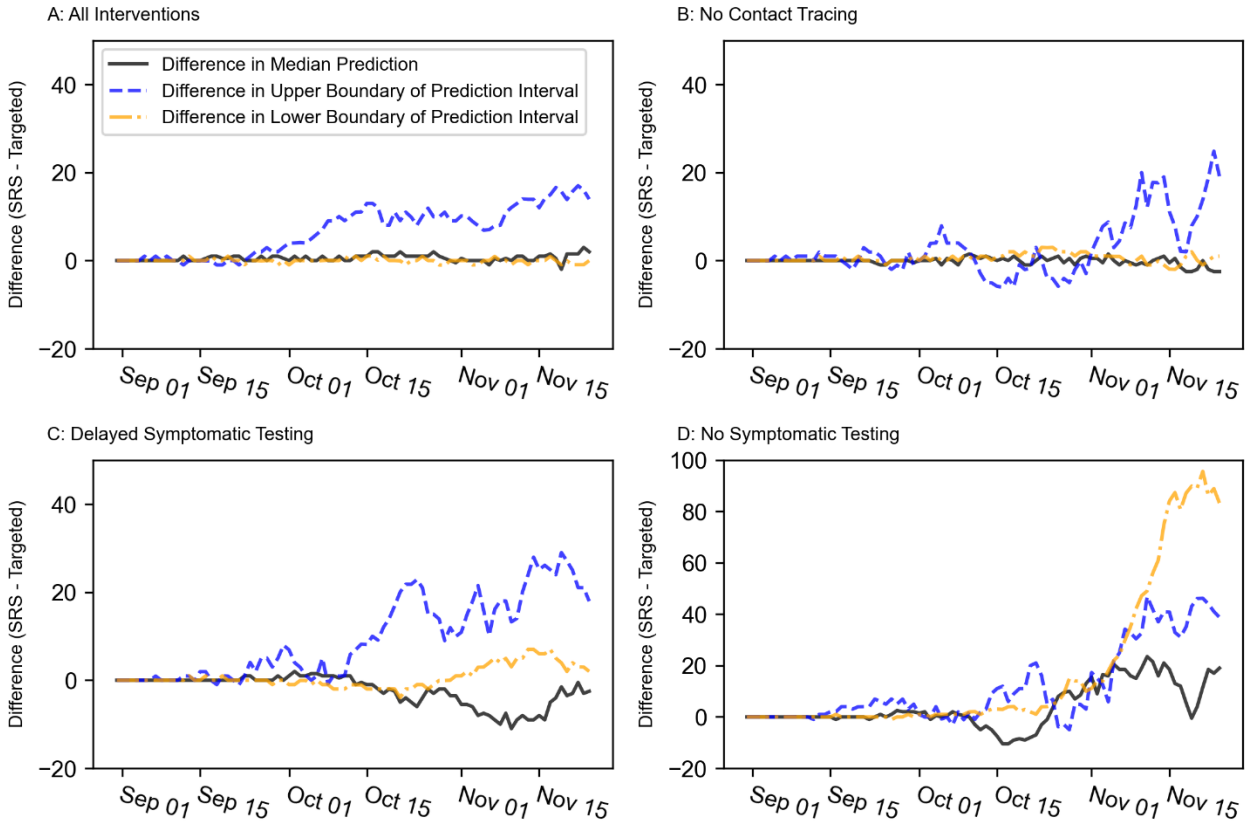

Fig 4. Differences between the cumulative infections under targeted sampling and SRS when other interventions are removed. Black, solid lines represent the difference between the median predicted cumulative infections under SRS and that under targeted sampling. Blue, dashed lines represent the difference between the 90% prediction interval's upper boundary under SRS and that under targeted

sampling. Gold, dashed-and-dotted lines represent the difference between the 90% prediction interval's lower boundary under SRS and that under targeted sampling. A) All-interventions scenario, B) No-contact-tracing scenario, C) Delayed-symptomatic testing scenario, D) No-symptomatic testing scenario

Discussion

Overview of university response

Like most IHEs, Quinnipiac University developed a plan to provide an in-person learning experience in fall 2020 while mitigating the spread of SARS-CoV-2. Given the novelty of COVID-19, there was limited data available to guide policy decisions. Therefore, the University extended an existing model of SARS-CoV-2 dynamics to help inform the University's COVID-19 policies. The modeling team devised, implemented, and updated a targeted sampling scheme to choose students for surveillance testing with the goal of quickly detecting and then responding to outbreaks within university residences. Finally, the University had a devoted team of contact tracers and asked students to actively monitor themselves for symptoms using a cellular phone application.

Many research groups housed across several universities used models of COVID-19 dynamics to inform university re-opening plans for fall 2020. These models utilized varied strategies, including not only agent-based models (14,31–34), but also models based on classic compartmental structures (e.g., (15,35–41)), network theory (22,42), and probability theory (43). Our agent-based model was a specially modified version of the Institute for Disease Modeling's Covasim model (16). Extending Covasim, rather than building our own model from scratch, allowed us to capitalize on a well-structured model of disease dynamics that incorporated the best estimates for epidemiological parameters that were available in summer 2020 (16). Our limited personnel could then focus on refining the model to account for social and epidemiological properties unique to our situation, such as the structure of university-owned residences.

Because the University's response to COVID-19 was so time sensitive, it would not have been feasible to develop such a complicated model without drawing on publicly available, open-source programs, and such programs could likely facilitate university responses to future EIDs and Disease X scenarios.

Even with the intellectual head start that the original Covasim provided us, certain policy decisions had to be made using versions of the model that lacked features described here. For instance, decisions about what sampling coverage to use for surveillance testing and whether to use our targeted sampling design rather than SRS had to be informed using a version of the model that only simulated residential students, did not incorporate dedensification in university-owned properties, and set the probability of transmission to Covasim's default value. Indeed, policy decisions made for spring 2020 and fall 2021 were informed using model features that were not described here because they were introduced in newer versions of Covasim (*e.g.*, waning immunity, vaccinations, and co-circulating strains (44)) or were created after fall 2020 (*e.g.*, a separate graduate student category for agents).

Model performance

One of the primary roles that our model played in Quinnipiac's COVID-19 response was to assess how disease properties that were not well understood in summer 2020 impacted case and infection rates. In the work described here, we explored four main scenarios that differed in basic reproductive number (R_0) and average contact rate: i) $R_0 = 1.5$, 8 contacts/day, ii) $R_0 = 1.5$, 10 contacts/day, iii) $R_0 = 2.5$, 8 contacts/day, iv) $R_0 = 2.5$, 10 contacts/day. No scenario universally fit the observed case incidence data well. The $R_0 = 1.5$, 10 contacts/day scenario performed adequately until a super-spreader event led to a sudden shock in the observed incidence rate on Nov. 8 (Fig 1B). The observed cumulative cases on and after Nov. 8 exceeded those predicted in every scenario. However, the University substantially increased its surveillance testing efforts during this period in response to the super-spreader event and moved to sampling all students on Nov. 15 (Table B in S1 Appendix). Since no scenario included this shift in effort, we would expect the observed case rate to exceed that of the model, even if the disease dynamics were

482 accurately simulated. However, the predicted cumulative infections provided an absolute cap on how
483 many diagnosed cases could have occurred in the model. Since the observed cumulative cases on and
484 after Nov. 8 remained within the prediction interval for cumulative infections under the $R_0 = 2.5$, 10
485 contacts/day scenario, the model may have still provided a reasonable approximation to disease dynamics
486 during this period (Fig 1D). Differences between the model's sampling rate and the achieved sampling
487 rate during testing may have also contributed to the model's tendency to overpredict the number of
488 reported cases early in the semester. Although the model's sampling rates and the requested sampling rate
489 during testing initially matched, frequently only around 70% of students selected for surveillance testing
490 actually responded.

491 It is noteworthy that both scenarios that fit the observed data best included an average of 10
492 contacts/day. Model-based estimates for the student contact rate at Villanova University were also around
493 10 contacts/day ([8.2020,10.9953]) (41), suggesting that this may be a reasonable approximation to
494 university student behavior under pandemic conditions. However, further estimates from a more diverse
495 set of IHEs are needed.

496 The scenarios' shifting fits indicate that the model may have performed better if model parameter
497 values were dynamic. As previously suggested, the $R_0 = 2.5$, 10 contacts/day scenario's 90% prediction
498 interval for cumulative diagnosed cases could have bounded the observed cases if the surveillance-testing
499 interventions' sampling rates had shifted within the simulation. Shifts in other model parameters could
500 have allowed a single scenario to accurately represent the University's disease dynamics and to better
501 capture the curvature in the observed cases' trajectory. Periods where parameter shifts would improve the
502 fit may reflect changes in the University's disease dynamics. The two best fitting scenarios used the same
503 contact rate but differed in R_0, which under the model's assumptions, suggests a shift in the probability of
504 transmission. Such a shift would occur, for instance, if students became lax toward public health policies
505 as the semester progressed (*e.g.*, violating the universal mask policy more frequently). In addition, the

R_0=2.5 scenario had a higher rate of imported infections, which may reflect the rising COVID-19 prevalence within the surrounding community as the semester progressed.

Alternatively, the model's fit may have also been improved by representing the super-spreader event as a sudden increase in the number of infections without any in-simulation transmission. This strategy would have emphasized the uniqueness of the super-spreader event as a violation of the University's usual disease dynamics. A compartmental model of COVID-19 transmission at Villanova University provided a better fit to observed case numbers when it was allowed to include similar shocks (41).

Relationship between IHEs and their surrounding communities

Both the observed cumulative cases and the model results underscore the interconnection between student populations and an IHE's surrounding community. The rate of imported infections is the model's primary representation of how the student body interacts with the surrounding community. The model's assumptions favor a proportional relationship between the final cumulative cases and the rate of imported infections. We therefore measured the model's sensitivity to the rate of imported infections using the slope of a least-squares line passing through the origin that relates the cumulative number of infections to the rate of imported infections. If the rate of imported infections had no net effect on local transmission, we would expect the line's slope to be 12.29 because there are 12.29 weeks (*i.e.*, 86 days) in each simulation. However, the slope exceeded this limit in every scenario. The model becomes more sensitive to the rate of imported infections at higher R_0 values and higher contact rates. In the R_0 = 1.5, 8 contacts/day scenario, one additional imported infection per week is estimated to cause 17.1 more infections by the end of the simulation, but the same increase is estimated to cause 27.6 more infections under the R_0 = 2.5, 10 contacts/day scenario. This latter slope is over twice the baseline rate of 12.3 infections, suggesting a significant role for on-campus-off-campus interactions in an IHE's disease dynamics. These findings corroborate results found in other models of IHE COVID-19 dynamics that

suggested that imported infections can have a major effect on an IHE's incidence rate or can hinder the effectiveness of an IHE's interventions (14,35,43) (though see (31)). Interestingly, Gressman and Peck (32) found nearly the same proportional relationship between the cumulative number of infections and the daily contact rate in their model as we found between the cumulative number of infections and the rate of imported infections under the $R_0 = 2.5$, 10 contacts/day scenario. The significance, if any, of this similarity is unclear, though.

Two key patterns in the observed cumulative cases suggest a linkage between campus disease dynamics and events in the surrounding community. First, after a low incidence rate in August and September, the University's rate considerably increased at the beginning of October (Fig 1). During this same interval, the case incidence in New Haven County, in which Quinnipiac is located, rose from an average of 26.73 new cases per day in September to 92.74 new cases per day in October, suggesting a possible relationship between community prevalence and campus prevalence (45). Although this study is not equipped to evaluate the nature of this proposed relationship, the roughly 7,100 students attending Quinnipiac in person during the fall 2020 semester is small relative to the 864,835 residents of New Haven County (11,46). Further, the case incidence in New Haven County had already begun to rise in September from an average of 20.45 cases per day in August (45). As a result, it seems likely that increases in the surrounding community's prevalence led to increases in the University's incidence rate and not vice-versa. This interpretation would be consistent with the rate of imported infection's sensitivity analysis since the estimated prevalence in the community partially determined this rate (S1 Appendix).

The second major pattern in the observed case data was the incidence's sudden increase after the late October super-spreader event (Fig 1). This event was associated with an off-campus Halloween party. Although student behavior was the core cause of the event, the event was also linked to alleged violations of state public health laws at a business in the surrounding community (47). So, despite being a campus-specific phenomenon, it arose from a combination of on-campus factors (*i.e.*, student behavior) and off-campus factors (*i.e.*, legal lapses in the community).

Here, we have focused on the role that the surrounding community may have played in increasing an IHE's case incidence rate, but both model-based and empirical evidence suggest that disease dynamics at IHEs can also increase the case and mortality rates in the surrounding community (48–51). Further research is needed to better understand this complex relationship, including under what conditions IHEs have a negative impact on surrounding communities and under what conditions surrounding communities have negative impacts on IHEs. Currently, compartmental model results suggest that surrounding communities have a larger role in augmenting incidence rates at IHEs when the IHE has effectively controlled transmission through public health interventions (35).

The interconnection between campuses and communities may challenge containment efforts in the face of future EIDs. Ultimately, IHE officials only have jurisdiction over the campus itself. As such, successful containment may require close collaboration between university and local, county, and state officials (48,52). Yet, the interconnection also means that information about the surrounding community can inform on-campus policies. For example, a university could increase surveillance testing or impose more stringent requirements to enter campus when community transmission is high.

Sampling strategy for surveillance testing

Like many IHEs, Quinnipiac conducted surveillance testing on the student body to detect asymptomatic and subclinical infections. Unlike most IHEs, residential students were sampled for surveillance testing using a targeted design that combined features of stratified and clustered sampling. The design's goal was to ensure even and consistent coverage across rooms, suites, and floors in university-owned properties, but the targeted design was partially extended to include externally owned properties if three or more non-residential students were known to share the address. Observed cases in university-owned properties did tend to cluster within rooms and floors, suggesting that our strategy likely did facilitate the discovery of case clusters. Further, we divided the student body into residential students, non-residential undergraduates, non-residential graduate students, and student athletes. Each

579 subpopulation received its own sampling rate. Because we had categorized students in this manner, we
580 were able to rapidly increase testing in subpopulations where we had identified increased case rates. We
581 were also able to determine whether any additional strategies employed to interrupt transmission in those
582 subpopulations were effective.

583 To the best of our knowledge, no other IHE used the same sampling strategy as Quinnipiac.
584 However, other universities had favorable results with similar targeted strategies. An Indiana university
585 used a stratified sampling design and adapted each stratum's sampling rate in response to new case data,
586 which likely contributed to the containment of a major outbreak (12). Similarly, empirical and model-
587 based evidence suggest that a targeted sampling design at Clemson University that focused surveillance
588 tests towards university-own residences that experienced a new case played an important role in
589 mitigating disease prevalence (15).

590 Simulation results suggest that our targeted sampling strategy and SRS would have had
591 comparable effects on the infection rate when contact tracing and app-based symptom monitoring were
592 also implemented (Fig 3). Complete sampling decreased the cumulative infections under every scenario,
593 but the degree of difference relative to targeted sampling depended on R_0. In the R_0=1.5 scenarios,
594 complete sampling reduced the median cumulative infections by no more than 24 infections, whereas the
595 median cumulative infections was reduced by at least 110 infections in both R_0=2.5 scenarios. Assuming
596 comparable results would occur using the effective reproductive number, these results validate the
597 University's strategy of shifting sampling rates based on current incidence data. If a university has limited
598 resources to test for an EID, a more economical strategy for surveillance testing may be to sample the
599 student population at a lower rate when the observed transmission rate is low because the reduction in
600 infections per test will also be lower. This would then reserve resources for increased sampling during
601 periods of high transmission when the reduction in infections per test is high. A similar strategy appeared
602 to provide favorable results at Furman University (13). This conclusion is similar to Paltiel *et al*. (39),
603 who found that the effective reproductive number altered what sampling frequency was most cost

effective, and to Hambridge, Kahn, and Onnela (34), who found that increasing the frequency of surveillance testing has smaller effects on the infection rate when R_0 is low than when it is high. A university using this adaptive sampling design would need to implement other public health interventions, though. The model results were predicated on contact tracing and app-based symptom monitoring's inclusion, and surveillance testing in the low-rate phase would predominantly monitor whether the rate needs to be shifted upward, so other inventions would be necessary to regulate transmission.

In the holdout scenarios, we withheld individual interventions in the model to explore each intervention's impact on a population of residential students. These results suggest that targeted sampling and SRS had comparable effects on the infection rate in our main epidemiological scenarios because other public health interventions were effectively controlling transmission. When either contact tracing or symptom monitoring was absent, the targeted strategy provided some benefit over SRS (Fig 4B-D). Interestingly, under most holdout scenarios, the major difference between strategies was in the upper boundary of the 90% prediction intervals rather than the median prediction. Given that complete sampling also had a greater impact on the upper boundary, the sampling strategy used for surveillance testing may have more value in mitigating the worst-case outcome than the typical outcome. Previous work has similarly suggested that the frequency of surveillance testing may have a greater role in controlling the maximum size of outbreaks than the average size (14). Which intervention is removed also influences targeted sampling's effect. In the no-contact-tracing and delayed-symptom-monitoring scenarios, targeted sampling had a noticeable but modest impact on the 90% prediction interval's upper boundary and no noticeable impact on the lower boundary or median prediction. In contrast, targeted sampling caused sizeable reductions in both the prediction interval's boundaries and even moderately reduced the median prediction.

App-based symptom monitoring as a containment strategy

Comparisons between the holdout scenarios under targeted sampling suggest that app-based symptom monitoring may have a high efficacy for controlling transmission. App-based symptom monitoring was assumed to reduce the expected waiting time between when a student developed symptoms and when the student sought testing and quarantined. We set this expected waiting time to one day in the main and all-intervention scenarios. The delayed-symptom-monitoring scenario assumed the symptom-monitoring application was missing, and the students' expected waiting times for testing were 4.82 days, the same as the general population (29). The median prediction for final cumulative infections under the all-interventions scenario had 179.5 fewer infections than that of the delayed-testing scenario. This difference is not only twice as great as that of the no-contact-tracing scenario but is even greater than the difference between targeted sampling and complete sampling under the R_0=2.5, 10 contacts/day scenario. App-based monitoring's apparent efficacy in the model results may arise because the symptom-monitoring application instructed symptomatic students to immediately quarantine after seeking testing but before receiving results; in contrast, surveillance testing and contact tracing both delayed quarantining until test results became available. Other models have found similar relationships between testing delays and surveillance testing's efficacy, either through increased effectiveness when testing is implemented more frequently (35,38,39) or when test results are returned more quickly (31,35,38,43). However, the actual impact that app-based monitoring had on the University's COVID-19 dynamics is less clear. Our model assumed every student faithfully used the application daily and would report symptoms to the app earlier than they would otherwise seek treatment. In reality, community uptake was limited, and no data is available on whether the application altered student behavior.

Role of non-residential students in disease transmission

Finally, since the R_0 = 2.5, 10 contacts/day and all-interventions scenarios were identical except for the inclusion of non-residential students in the former, a comparison between the two provides insights into the role that non-residential students may have played in disease transmission. Even though

residential students comprised 49.0% of the student population in the R_0 = 2.5, 10 contacts/day scenario, the cumulative infections under the all-interventions scenario was 38.9% that of the R_0 = 2.5, 10 contacts/day scenario after subtracting the expected number of imported infections from each scenario's cumulative infections. This suggests that non-residential students have a disproportional impact on a university's local transmission. Indeed, the University's observed testing data supported this hypothesis. The gradual case increases that began in the first week of October were due to an increase in cases in non-residential students. Other universities also witnessed higher case rates in non-residential students than their residential peers, although the relative sizes of these subpopulations were not always clear (9,12). In these scenarios, non-residential students may have experienced high infection rates through a combination of increased mixing with the surrounding community and decreased oversight from the University's public health team. However, this pattern was far from universal, and other universities reported a disproportional number of cases in their residential populations, although the difference was not always statistically significant (10,13,15).

Implication for future emerging infectious diseases

The implications these results have for future EID outbreaks is complicated. App-based symptom monitoring heavily reduced the infection rate in the model and requires few resources to implement. Further, because symptom monitoring is a strategy that translates to most diseases, app-based symptom monitoring would be relatively easy to launch in the face of a new Disease X scenario. Yet, individual students are responsible for monitoring their own health under this intervention, and as the late October super-spreader event and comparable events at other universities (*e.g.*, (12,13,41)) illustrate, student behavior can be difficult to predict. A website-based symptom monitoring program failed to prevent a major outbreak at an Indiana university (12). University officials may have more success with app-based monitoring if they include measures to encourage adherence. Indeed, the Indiana university attributed their successful containment efforts partially to a public health educational campaign (12), and model-

based results indicate that educational programs can decrease infection rates when combined with other interventions (38). In any case, app-based symptom monitoring would need to be used in conjunction with other interventions in a Disease X scenario, as its effectiveness will depend on disease-specific rates and severities of symptoms.

Contact tracing was also effective in controlling the transmission rate in simulated results. This intervention has a long and proven track record in public health policy, translates well to novel diseases, and was found to have a comparable effectiveness to surveillance testing with complete sampling in other modeling studies of COVID-19 (41). However, contact tracing requires trained personnel that may not be available at every university.

Finally, like numerous other modeling studies (*e.g.*, (39,41)), we found that surveillance testing with complete sampling can substantially decrease infection rates. Complete sampling requires a vast amount of financial, logistical, and human resources to implement, though, and cannot be launched in Disease X situations until reliable tests are developed. Many universities will not have the means to make this strategy feasible. Even when complete sampling is infeasible, though, targeted sampling and SRS can still assist in outbreak detection at a significantly reduced cost, as it did for Quinnipiac. Although the model results found that the use of targeted sampling to obtain students for surveillance testing did not impact the infection rate differently than SRS, there are still reasons why a university might choose to use targeted sampling in the face of an EID or Disease X scenario. First, the holdout scenarios suggested that targeted sampling does control worst-case infection rates better than SRS when the delay between developing symptoms and testing is increased. This suggests that targeted testing's relative advantage depends on features of the disease's presentation, such as the severity of illness, the rate of asymptomatic infections, and degree of infectiousness before symptom onset. These properties are variable between diseases and may not be well-understood early in an EID outbreak. Targeted testing does not require many more resources than SRS, so a university might elect to use targeted sampling to capitalize on any potential benefits with little penalty. Second, the even sampling coverage that targeted testing provides

can help to reassure students, faculty, staff and parents that a campus is safely opening. Although not directly related to disease progression, the reduction in anxiety and stress could yield significant mental health benefits.

Disease X scenarios pose major threats to global public health because policy responses need to be made before a substantial amount of information is available about the disease. COVID-19 was one example of such a scenario, so careful documentation and study of how institutions, such as IHEs, responded to COVID-19 could improve responses to future Disease X scenarios. Here, we described Quinnipiac University's response and its effectiveness. However, IHEs contain diverse populations and exist in varied contexts that can influence an intervention's effect. For example, Quinnipiac University and Furman University launched comparable COVID-19 responses (*e.g.*, app-based symptom monitoring, adaptive sampling rates for surveillance testing), but the case data for the two universities sometimes yielded contradictory patterns (*e.g.*, the proportion of off-campus students in the case data) (13). Thus, one major limitation to this study is the limited scope of its population. A more thorough review of IHE responses and their effectiveness would help to build more robust responses. Although some attempts have been made to create such a review (49), limited and inconsistent documentation across IHEs have stifled these efforts. A second major limitation is that COVID-19 is just one Disease X scenario. The next Disease X may have very different medical and epidemiological properties to COVID-19 and strategies effective for COVID-19 may not be effective in these scenarios. Public health and IHE officials will therefore need to remain flexible when preparing for future EIDs and Disease X scenarios and build contingency plans into their responses to account for differential effectiveness.

Acknowledgements

The authors would like to thank the Quinnipiac University COVID-19 Task Force for supporting the modeling efforts, to the faculty and staff for their assistance in data collection, to N Bharti for providing us with a preprint of her and her collaborator's manuscript on university-based contact tracing data, as

well as M Ferrari for introducing us to N Bharti, and CC Kerr and the Institute for Disease Modeling for access to the Covasim model.

Author Contributions

Conceptualization: K. James Soda, Xi Chen, Richard Feinn, David R. Hill

Formal Analysis: K. James Soda

Methodology: K. James Soda, Xi Chen, Richard Feinn, David R. Hill

Project Administration: Richard Feinn, David R. Hill

Software: K. James Soda

Visualization: K. James Soda, Xi Chen

Writing-Original Draft Preparation: K. James Soda, Xi Chen, Richard Feinn, David R. Hill

Writing- Review & Editing: K. James Soda, Xi Chen, Richard Feinn, David R. Hill

References

1. World Health Organization. Regional Office for South-East Asia. Combating Emerging Infectious Diseases in the South-East Asia Region. WHO Regional Office for South-East Asia. 2005. Available from: https://apps.who.int/iris/handle/10665/204878.
2. Morens DM, Fauci AS. Emerging Pandemic Diseases: How We Got to COVID-19. Cell. 2020;182(5):1077–92. doi: 10.1016/j.cell.2020.08.021
3. Jones KE, Patel NG, Levy MA, Storeygard A, Balk D, Gittleman JL, et al. Global trends in emerging infectious diseases. Nature. 2008;451(7181):990–3.
4. Morens DM, Daszak P, Taubenberger JK. Escaping Pandora's Box — Another Novel Coronavirus. N Engl J Med. 2020;382(14):1293–5.
5. Holmes BEC. COVID-19— lessons for zoonotic disease. Science. 2022;375(6585):1114–5.
6. Iserson K V. The next pandemic: Prepare for "Disease X." West J Emerg Med. 2020;21(4):756–8.
7. The WHO R&D Blueprint Team. Prioritizing diseases for research and development in emergency contexts. 2022 [cited 2022 Jul 9]. In: World Health Organization [Internet]. Geneva: World Health

Organization. [about 2 screens]. Available from: https://www.who.int/activities/prioritizing-diseases-for-research-and-development-in-emergency-contexts

8. Morens DM, Breman JG, Calisher CH, Doherty PC, Hahn BH, Keusch GT, et al. The Origin of COVID-19 and Why It Matters. Am J Trop Med Hyg. 2020;103(3):955–9.

9. Vang KE, Krow-Lucal ER, James AE, Cima MJ, Kothari A, Zohoori N, et al. Participation in Fraternity and Sorority Activities and the Spread of COVID-19 Among Residential University Communities — Arkansas, August 21–September 5, 2020. MMWR Morb Mortal Wkly Rep. 2021;70(1):20–3.

10. Wilson E, Donovan C V, Campbell M. Multiple COVID-19 Clusters on a University Campus —. MMWR Morb Mortal Wkly Rep. 2020;69(39):1416–8.

11. US News & World Reports. Quinnipiac University Student Life. US News & World Reports. 2022 [cited 2022 Jul 12]. Available from: https://www.usnews.com/best-colleges/quinnipiac-university-1402/student-life

12. Fox MD, Bailey DC, Seamon MD, Miranda ML. Response to a COVID-19 Outbreak on a University Campus — Indiana, August 2020. MMWR Morb Mortal Wkly Rep. 2021;70(4):118–22.

13. Cass AL, Slining MM, Carson C, Cassidy J, Carmela Epright M, Gilchrist AE, et al. Risk management of COVID-19 in the residential educational setting: Lessons learned and implications for moving forward. Int J Environ Res Public Health. 2021;18(18).

14. Goyal R, Hotchkiss J, Schooley RT, De Gruttola V, Martin NK. Evaluation of Severe Acute Respiratory Syndrome Coronavirus 2 Transmission Mitigation Strategies on a University Campus Using an Agent-Based Network Model. Clin Infect Dis. 2021;73(9):1735–1741.

15. Rennert L, McMahan C, Kalbaugh CA, Yang Y, Lumsden B, Dean D, et al. Surveillance-based informative testing for detection and containment of SARS-CoV-2 outbreaks on a public university campus: an observational and modelling study. Lancet Child Adolesc Heal. 2021;5:428–36. doi: 10.1016/S2352-4642(21)00060-2

16. Kerr CC, Stuart RM, Mistry D, Abeysuriya RG, Hart G, Rosenfeld K, et al. Covasim : an agent-based model of COVID-19 dynamics and interventions. PLoS Comput Biol. 2021;17(7):e1009149.

17. Axelrod R. The Complexity of Cooperation: Agent-Based Models of Competition and Collaboration. Princeton, NJ: Princeton University Press; 1997.

18. Panovska-Griffiths J, Kerr CC, Stuart RM, Mistry D, Klein DJ, Viner RM, et al. Determining the optimal strategy for reopening schools, the impact of test and trace interventions, and the risk of occurrence of a second COVID-19 epidemic wave in the UK : a modelling study. Lancet Child Adolesc Heal. 2020;4(11):817–27. doi: 10.1016/S2352-4642(20)30250-9

19. Panovska-Griffiths J, Stuart RM, Kerr CC, Rosenfeld K, Mistry D, Waites W, et al. Modelling the impact of reopening schools in the UK in early 2021 in the presence of the alpha variant and with roll-out of vaccination against SARS-CoV-2. J Math Anal Appl. 2022;514(2):126050.

20. Panovska-Griffiths J, Kerr CC, Waites W, Stuart RM, Mistry D, Foster D, et al. Modelling the potential impact of mask use in schools and society on COVID-19 control in the UK. Sci Rep. 2021;11:8747. doi: 10.1038/s41598-021-88075-0

21. Cohen JA, Mistry D, Kerr CC, Klein DJ. Schools are not islands: Balancing COVID-19 risk and educational benefits using structural and temporal countermeasures. medRxiv: 2020.09.08.20190942 [Preprint]. 2020 [cited 2023 Jan 8]. Available from: https://www.medrxiv.org/content/10.1101/2020.09.08.20190942v1%0Ahttps://www.medrxiv.org/content/10.1101/2020.09.08.20190942v1.abstract

22. McAlpine KJ. The story, and the science, behind BU's COVID-19 dashboard. 2020 Aug 27 [cited 2023 Jan 1]. In: The Brink [Internet]. Boston: Boston University. [about 23 screens]. Available from: https://www.bu.edu/articles/2020/the-story-the-science-behind-bu-covid-19-dashboard/

23. Kuhfeldt K, Turcinovic J, Sullivan M, Landaverde L, Doucette-Stamm L, Hamer DH, et al. Examination of SARS-CoV-2 In-Class Transmission at a Large Urban University with Public Health Mandates Using Epidemiological and Genomic Methodology. JAMA Netw Open.

2022;5(8):e2225430.

24. U.S. Census Bureau. 2018: ACS 1-Year Estimates Subject Tables; 2018 [cited 2023 Jan 8]. Database: data.census.gov [Internet]. Available from: https://data.census.gov/cedsci/table?q=age distribution 2018&tid=ACSST1Y2018.S0101

25. Hanson KE, Caliendo AM, Arias CA, Englund JA, Lee MJ, Loeb M, et al. Infectious Diseases Society of America Guidelines on the Diagnosis of Coronavirus Disease 2019. Clin Infect Dis. 2020 Jun 16;ciaa760. doi: 10.1093/cid/ciaa760

26. Bharti N, Exten C, Fulton V, Oliver-Veronesi R. Lessons from campus outbreak management using test, trace, and isolate efforts. Am J Infect Control. 2021;49(6):849–51.

27. Virtanen P, Gommers R, Oliphant TE, Haberland M, Reddy T, Cournapeau D, et al. SciPy 1.0: fundamental algorithms for scientific computing in Python. Nat Methods. 2020;17(3):261–72.

28. Branch MA, Coleman TF, Li Y. Subspace, interior, and conjugate gradient method for large-scale bound-constrained minimization problems. SIAM J Sci Comput. 1999;21(1):1–23.

29. Khalili M, Karamouzian M, Nasiri N, Javadi S, Mirzazadeh A, Sharifi H. Epidemiological Characteristics of COVID-19; a Systemic Review and Meta-Analysis. Epidemiol Infect. 2020;148(e130):1–17.

30. National Center for Immunization and Respiratory Diseases (NCIRD), Division of Viral Diseases. Overview of Testing for SARS-CoV-2, the virus that causes COVID-19. 2022 Sept 28 [cited 2022 Oct 9]. In: COVID-19 [Internet]. Atlanta: Centers for Disease Control and Prevention. [about 18 screens]. Available from: https://www.cdc.gov/coronavirus/2019-ncov/hcp/testing-overview.html

31. Bahl R, Eikmeier N, Fraser A, Junge M, Keesing F, Nakahata K, et al. Modeling COVID-19 spread in small colleges. PLoS One. 2021;16(8):e0255654. doi: 10.1371/journal.pone.0255654

32. Gressman PT, Peck JR. Simulating COVID-19 in a university environment. Math Biosci. 2020;328:108436. doi: 10.1016/j.mbs.2020.108436

33. Cator D, Huang Q, Ndeffo-mbah M, Mondal A, Lee S, Gurarie D. Individual-based modeling of COVID-19 transmission in college communities. Math Biosci Eng. 2022; 13861-77.

827 34. Hambridge H, Kahn R, Onnela J. Efficacy of SARS-CoV-2 repeat testing to control spread in
828 residential college populations. Int J Infect Dis. 2021;113:325–30.
829 35. Lopman B, Liu CY, Le Guillou A, Handel A, Lash TL, Isakov AP, et al. A modeling study to
830 inform screening and testing interventions for the control of SARS-CoV-2 on university campuses.
831 Sci Rep. 2021;11:5900. doi: 10.1038/s41598-021-85252-z
832 36. Rennert L, Kalbaugh CA, Shi L, McMahan C. Modelling the impact of presemester testing on
833 COVID-19 outbreaks in university campuses. BMJ Open. 2020;10:e042578.
834 37. Zhao X, Tatapudi H, Corey G, Gopalappa C. Threshold analyses on combinations of testing,
835 population size, and vaccine coverage for COVID-19 control in a university setting. PLoS One.
836 2021;16(8):e0255864. doi: 10.1371/journal.pone.0255864
837 38. Ghaffarzadegan N. Simulation-based what-if analysis for controlling the spread of Covid-19 in
838 universities. PLoS One . 2021;16(2):e0246323. doi: 10.1371/journal.pone.0246323
839 39. Paltiel AD, Zheng A, Walensky RP. Assessment of SARS-CoV-2 Screening Strategies to Permit
840 the Safe Reopening of College Campuses in the United States. JAMA Netw Open.
841 2020;3(7):e2016818.
842 40. Martin NK, Schooley RT, De Gruttola V. Modelling testing frequencies required for early
843 detection of a SARS-CoV-2 outbreak on a university campus. medRxiv: 2020.06.01.20118885
844 [Preprint]. 2020 [cited 2023 Jan 8]. Available from:
845 https://www.medrxiv.org/content/10.1101/2020.06.01.20118885v1.full.pdf
846 41. Muller K, Muller PA. Mathematical modelling of the spread of COVID-19 on a university
847 campus. Infect Dis Model. 2021;6:1025–45. doi: 10.1016/j.idm.2021.08.004
848 42. Borowiak M, Ning F, Pei J, Zhao S, Tung HR, Durrett R. Controlling the spread of COVID-19 on
849 college campuses. Math Biosci Eng. 2021;18(1):551–63.
850 43. Chang JT, Crawford FW, Kaplan EH. Repeat SARS-CoV-2 testing models for residential college
851 populations. Health Care Manag Sci. 2021;24(2):305–18.
852 44. Cohen JA, Stuart RM, Rosenfeld K, Lyons H, White M, Kerr CC, et al. Quantifying the role of

naturally- and vaccine-derived neutralizing antibodies as a correlate of protection against COVID-19 variants. medRxiv: 2021.05.31.21258018 [Preprint]. 2021 [cited 2023 Jan 8]. Available from: https://www.medrxiv.org/content/10.1101/2021.05.31.21258018v2%0Ahttps://www.medrxiv.org/content/10.1101/2021.05.31.21258018v2.abstract

45. Covid Act Now. Covid Act Now API; 2022 [cited 2022 Jul 21]. Database: COVID Act Now [Internet]. Available from: https://apidocs.covidactnow.org/

46. U.S. Cenus Bureau. 2020: DEC Redistricting Data (PL 94-171); 2021 [cited 2022 Jul 28]. Database: census.gov [Internet]. Available from: https://www.census.gov/quickfacts/newhavencountyconnecticut

47. O'Leary ME. New Haven closes Anthony's Ocean View due to alleged COVID violations. New Haven Registrar. 2020 Oct 30 [cited 2022 Jul 12]. Available from: https://www.nhregister.com/news/article/New-Haven-closes-Anthony-s-Ocean-View-due-to-15689827.php

48. Cipriano LE, Haddara WMR, Zaric GS, Enns EA. Impact of university re-opening on total community COVID-19 burden. PLoS One. 2021;16(8 August):1–16. doi: 10.1371/journal.pone.0255782

49. Klein B, Generous N, Chinazzi M, Bhadricha Z, Gunashekar R, Kori P, et al. Higher education responses to COVID-19 in the United States: Evidence for the impacts of university policy. PLOS Digit Heal. 2022;1(6):e0000065. doi: 10.1371/journal.pdig.0000065

50. Mangrum D, Niekamp P. JUE Insight: College student travel contributed to local COVID-19 spread. J Urban Econ. 2022;127(May 2020):103311. doi: 10.1016/j.jue.2020.103311

51. Lu H, Weintz C, Pace J, Indana D, Linka K, Kuhl E. Are college campuses superspreaders? A data-driven modeling study. Comput Methods Biomech Biomed Engin. 2021;24(10):1136–45. doi: 10.1080/10255842.2020.1869221

52. Walke HT, Honein M, Redfield RR. Preventing and Responding to COVID-19 on College Campuses. JAMA. 2020;324(17):1727–8.

Supporting information

S1 Appendix. Derivation of model parameters and detailed targeted sampling description.

S2 Supporting Information. Python and R scripts to replicate the analyses in this paper.

S1 Appendix. Derivation of model parameters and detailed targeted sampling description.

Estimating the Rate of Imported Infections and COVID-19 Prevalence.

In the modified version of Covasim used in our study, the number of imported infections on each day is a Poisson random variable whose rate parameter differs between the residential and non-residential sub-populations. Under the assumption that the community surrounding the university is well mixed, the rate parameter for sub-population i (λ_i) was assumed to be:

$$\lambda_i = n_i c_i p \beta \quad (1)$$

Here, n_i is the size of sub-population i, c_i is the expected number of contacts between one student in sub-population i and non-student members of the community, p is the COVID prevalence in the university's surrounding community, and β is the base transmission probability. Whereas n_i and β were already parameters within the model, c_i and p required additional specification.

To determine reasonable values for c_i, we established the average number of contacts that each student will have in a day, excluding roommates, based on empirical estimates in Bharti et al. (1), then allocated these contacts to the in-simulation contact pools and to out-of-system community members. For residential students, contacts were predominantly allocated to the in-system pools; only one contact per day or one contact every other day was allocated to out-of-system individuals (Table 2 in main text). In contrast, non-residential students used the same number of community contacts as residential students, but all remaining contacts were allocated to out-of-system individuals. Here, we assumed individuals living outside of university-owned properties were more likely to interact with non-students.

Within this study, the area surrounding the university was defined as the entire state of Connecticut. Then, case incidence data led to rough estimates for p. All case incidence data came from COVID Act Now and were smoothed as seven-day averages (2). To estimate p, we decomposed the

number of infectious individuals on a given day (N_{it}) into the number of symptomatic individuals (N_{st}), the number of asymptomatic individuals (N_{at}), and the number of pre-symptomatic individuals (N_{pt}). We assumed there was a fixed probability that a symptomatic resident of Connecticut led to a reported case on any given day (p_d) and that only symptomatic individuals contribute to the reported incidence rate. Under these assumptions, the number of days between symptom onset and detection is a geometric random variable, but in some cases, the symptomatic individual will recover before being detected. Therefore, the probability that a symptomatic infection will eventually lead to a reported case ($p_{D|S}$) would be the following:

$$p_{D|S} = \sum_{i=1}^{T} p_d(1-p_d)^{i-1} \quad (2)$$

Here, T is the duration between symptom onset and recovery. Furthermore, define the reporting rate (ρ) as the probability that a randomly selected infection, be it symptomatic or asymptomatic, will lead to a reported case. Under this definition, $\rho = p_{D|S}p_S$, where p_S is the probability that an infection will be symptomatic.

Based on Khalili *et al.* (3), we set T to 18 days. Furthermore, CDC seroprevalence studies in Connecticut estimated that between 12.82% and 23.26% of all infections led to a reported case (4); therefore, we set ρ to 0.20. Finally, we set p_S to 0.6 based on Oran and Topol (5). Based on these estimates and Equation 2, we used numerical optimization algorithms in R ver. 4.2 to solve for p_d under the constraint that the value must be between 0 and 1 (6) (S2 Supporting Information). The estimated value was 0.022274.

The previous assumptions further imply that the total number of reported cases on a given day is a binomial random variable where the number of trials is N_{st} and the probability of success is p_d. Since the binomial distribution is unimodal, we estimated N_{st} as the integer value that places the distribution's mode

at the observed number of reported cases on day t ($n_{cases,t}$) under a strategy akin to maximum estimation. The mode of this binomial distribution is $\lfloor (N_{st}+1)p_d \rfloor$, where $\lfloor ... \rfloor$ is the floor function, so the estimate was roughly:

$$\widehat{N}_{st} = \frac{n_{cases,t}}{p_d} - 1 \quad (3)$$

The remaining estimates for N_{at} and N_{pt} followed from $\widehat{N}_{st}$. Since:

$$p_s \approx \frac{N_{st}}{N_{st} + N_{at}} \quad (4)$$

An approximate estimate for N_{at} is:

$$\widehat{N}_{at} = N_{st}\frac{1-p_s}{p_s} \quad (5)$$

Finally:

$$\widehat{N}_{pt} = \sum_{j=1}^{d} \left(\widehat{N}_{at+j} + \widehat{N}_{st+j} \right) \quad (6)$$

Where d is the duration between when an individual becomes infectious and when the individual develops symptoms, assuming a symptomatic infection. Based on Tindale *et al.* (7), we set d to three days. Our method for estimating N_{pt} represents an upper limit, though, as it assumes that symptomatic individuals or individuals that could be established as asymptomatic on day i do not overlap with those same groups on day (i + 1). Finally, to convert these estimates to a final prevalence for the state of Connecticut, the estimates were summed and divided by the estimated population of Connecticut according to the US

Census Bureau's July 1, 2019 estimate (8). R code for implementing these calculations is available in S2 Supporting Information.

Derivation of a Relationship Between R_0 and the Probability of Transmission.

Covasim does not explicitly use the basic reproductive number (R_0) as a model parameter. The closest analog is the base probability of transmission (β). Yet, because R_0 is a prominent parameter in public health guidelines, there is a utility to linking β to an *a priori* value for R_0 in a manner that is consistent with Covasim's assumptions and its default values for epidemiological parameters. Assume that there is a well-mixed population of susceptible individuals, that this population is arbitrarily large, and that disease transmission occurs in a manner identical to its depiction in Covasim. Define R_0 as the expected number of new infections in this population that directly result from introducing a single infectious individual. Since the population is arbitrarily large and well-mixed, the probability that the infectious individual will contact the same susceptible individual twice is approximately zero. Therefore, under Covasim's assumptions on disease transmission, the number of new infections depends on the total number of contacts the infectious individual makes before recovery and on the probability of transmission. Further, every contact is a Bernoulli trial that ends in either transmission or no transmission. Therefore, R_0 is the sum of the expected probability of transmission for each contact.

The probability of transmission for each contact is the product of β and two scaling factors. The first factor represents the relative susceptibility of the contacted individual (s_j), which is age-dependent (Table A) (9). Therefore, the expected susceptibility is the sum of each age group's susceptibility weighted by the proportion of the population that belongs to that age group. To establish this expected value, we used the age distribution of the entire US population rather than the population of the university, as this made our definition of R_0 more consistent with that of the broader literature (Table A).

974

975 **Table A.** The susceptibility constants associated with each age group in Covasim's defaults, as well as
976 the proportion of the US population that belongs to each age group (10).

Age Group	Susceptibility Constant	Proportion of the US Population
0-9	0.34	0.121
10-19	0.67	0.131
20-59	1	0.525
60-69	1.24	0.1095*
+70	1.47	0.1135*

977 * These values slightly differ from the proportions in (10). There, the population proportion in the 60-69
978 age group is 0.115, and the population proportion in the over 70 age group is 0.108. The values have been
979 left as-is for consistency with the model used in fall 2020. Correcting this difference minorly changes the
980 relationship to $\beta \approx \frac{R_0}{8.083054 n_c}$ and does alter β by more than $6\text{x}10^{-5}$.

981

982 The second scaling factor represents the relative transmissibility of the infectious individual at the time of
983 contact (r_{it}), which accounts for the infectious individual's viral load. Covasim's defaults assume that, in
984 most cases, the transmissibility scaling factor is two during the first 30% of the infectious period and one
985 during the final 70%. Assuming this generalization holds for the infectious individual, R_0 can be
986 expressed as the sum of the expected number of new infections during the first 30% of the infectious
987 period and the expected number during the last 70%, which simplifies subsequent calculations. The
988 duration of a simulated infectious period is a log normal random variable that depends on health

989 outcomes, such as whether an individual is asymptomatic or symptomatic, whether the individual requires
990 hospitalization, and whether the individual requires admission to an intensive-care unit. We assumed the
991 infectious period was nine days long, which is Covasim's default expected duration for an asymptomatic
992 infection or a symptomatic infection that does not require hospitalization. Since the model uses a one-day
993 timestep, this means that the period of elevated transmissibility lasts two days whereas the period of lower
994 transmissibility lasts seven days. In addition to viral load, r_{it} is further scaled by a random constant that is
995 unique to that individual (c_i), which accounts for idiosyncratic factors (*e.g.*, comorbid conditions, genetic
996 factors, behavioral factors). Since $100c_i \sim NegBinom\left(0.45, {}^{0.45}/_{100.45}\right)$, $\mathrm{E}[c_i]=1$.

997 Put together:

998 $$R_0 = \mathrm{E}\left[2\left(n_{c,h}c_i s_j \beta\right) + n_{c,l}c_i s_j \beta\right] = (2\mathrm{E}\left[n_{c,h}\right] + \mathrm{E}\left[n_{c,l}\right])\mathrm{E}[c_i]\mathrm{E}\left[s_j\right]\beta$$

999 Here, $n_{c,h}$ is the number of contacts the infectious individual has during the first 30% of the infectious
1000 period, $n_{c,l}$ is the number of contacts the infectious individual has during the final 70% of the infectious
1001 period, and all other parameters are as defined above. Notice that although $n_{c,h}$, $n_{c,l}$, c_i, and s_j are all
1002 random variables, they are all mutually independent, so the second equality holds. Recalling that the
1003 model assumes that the number of contacts an individual has in one day is a Poisson random variable,
1004 $\mathrm{E}[n_{c,h}]$ and $\mathrm{E}[n_{c,l}]$ are the expected number of contacts in one day times the duration of each parameter's
1005 associated period. Adding the assumption that the infectious period is nine days, the expression can be
1006 rearranged to provide an approximate relationship between R_0 and β when the expected number of
1007 contacts (n_c) is known:

1008 $$\beta \approx \frac{R_0}{8.766238 n_c}$$

1009 R code for implementing these calculations is available in S2 Supporting Information.

1010

Detailed Sampling Strategy.

All students had to provide confirmation of a negative COVID test in late August prior to the start of the fall semester and were tested again on campus at the beginning of the semester. After this, a targeted sampling plan for weekly COVID testing began.

Residential Undergraduate Students

We applied a strict stratified and cluster sampling method to students in residential dormitory buildings. Dormitories at Quinnipiac University have varied floor plans. Some dormitories contain typical student dorm rooms along a hallway, while other buildings have suites in which students share a living area and bathrooms but have separate bedrooms. Since students in the same suite lived in such close proximity, though, suites were treated as if they were a single dorm room. Similarly, the university owns multiroom houses that serve as student residences, but because students in the same house frequently contacted each other, QU-owned houses were treated comparably to a single dorm room. Occupancy per room varies largely by building, suite, or house. Starting in the fall of 2020, the university allowed a maximum of two students per dorm room. To guarantee at least one student from a close-contact living space was selected, we defined building floors (*i.e.*, those containing dorm rooms) and houses as strata in stratified sampling. We utilized a proportionate sampling method to determine the number of students being selected from each stratum and then used cluster sampling to draw students from dorm rooms, suites, and houses.

Non-Residential Undergraduate Students

About 40% of undergraduate students commuted to school. They either lived with relatives or rented an apartment or house in the local community. Since they had greater exposure to the community, the plan was to sample 25% of non-residential undergraduates each week. Based on student records, we could determine the number of students who shared an address. Students who shared an address with no more than one other student were entered in a pool for simple random sampling (SRS). Students who

shared the same address with two or more students (*i.e.*, the residence contained at least three students), including those living in the same apartment building as other students, were kept in a separate pool from which at least one student was selected weekly to be tested.

Graduates and Student Athletes

We assumed that graduate students, even those living off campus, would be more responsible and exhibit more precautious behaviors than undergraduates. Thus, we used SRS with a smaller sampling rate of 15%. However, graduate students who shared the same residence with undergraduate students or who lived in university-owned properties were placed in the undergraduate student pool and sampled in the same way as undergraduate students. Finally, we sampled 80% of student athletes weekly to meet the requirements set by the Metro Atlantic Athletic Conference of the National Collegiate Athletic Association. Student athletes were stratified by team.

Table B. Weekly proportion of students sampled and case incidence for each week.

		Sampling Percentages			
Week Ending Day	**Case Incidence**	**Res Undergrad**	**Non-res Undergrad**	**Graduate**	**Athletes**
Pre-arrival	-	100%	100%	100%	100%
08/30/2020	-	100%	100%	100%	100%
09/06/2020	2	100%	100%	100%	100%
09/13/2020	0	15%	25%	15%	80%
09/20/2020	1	15%	25%	15%	80%
09/27/2020	0	15%	25%	15%	80%
10/04/2020	3	15%	25%	15%	80%
10/11/2020	20	15%	35%	15%	80%
10/18/2020	7	15%	35%	15%	80%
10/25/2020	18	15%	35%	15%	80%
11/01/2020	48	15%	60%	40%	80%
11/08/2020	296	15%	60%	40%	80%
11/15/2020	151	100%	100%	100%	100%
11/22/2020	67	25%	25%	15%	80%

Res Undergrad = Residential undergraduate students, Non-res Undergrad = Non-residential undergraduate students, Graduate = Non-residential graduate students, Athletes = Student athletes

References

1. Bharti N, Exten C, Fulton V, Oliver-Veronesi R. Lessons from campus outbreak management using test, trace, and isolate efforts. Am J Infect Control. 2021;49(6):849–51.

2. Covid Act Now. Covid Act Now API; 2022 [cited 2022 Jul 21]. Database: COVID Act Now [Internet]. Available from: https://apidocs.covidactnow.org/

3. Khalili M, Karamouzian M, Nasiri N, Javadi S, Mirzazadeh A, Sharifi H. Epidemiological Characteristics of COVID-19; a Systemic Review and Meta-Analysis. Epidemiol Infect. 2020;148(e130):1–17.

4. Havers FP, Reed C, Lim T, Montgomery JM, Klena JD, Hall AJ, et al. Seroprevalence of Antibodies to SARS-CoV-2 in Six Sites in the United States, March 23-May 3, 2020. JAMA Intern Med. 2020;180(12):1576–86.

5. Oran DP, Topol EJ. Prevalence of Asymptomatic SARS-CoV-2 Infection. Ann Intern Med. 2020;173(5):362–7.

6. R Core Team. R: A Language and Environment for Statistical Computing [Internet]. Vienna, Austria; 2022. Available from: https://www.r-project.org/

7. Tindale L, Coombe M, Stockdale JE, Garlock E, Lau WYV, Saraswat M, et al. Transmission interval estimates suggest pre-symptomatic spread of COVID-19. medRxiv: 2020.03.03.20029983 [Preprint]. 2020 [cited 2023 Jan 9]. Available from: https://www.medrxiv.org/content/10.1101/2020.03.03.20029983v1.full.pdf

8. U.S. Census Bureau. 2019: PEP Population Estimates; 2019 [cited 2023 Jan 9]. Database: data.census.gov [Internet]. Available from: https://data.census.gov/cedsci/table?g=0400000US09&tid=PEPPOP2019.PEPANNRES

9. Kerr CC, Stuart RM, Mistry D, Abeysuriya RG, Hart G, Rosenfeld K, et al. Covasim : an agent-based model of COVID-19 dynamics and interventions. PLoS Comput Biol. 2021;17(7):e1009149.

10. U.S. Cenus Bureau. 2020: DEC Redistricting Data (PL 94-171); 2021 [cited 2022 Jul 28]. Database: census.gov [Internet]. Available from: https://www.census.gov/quickfacts/newhavencountyconnecticut